

## LETTER TO THE EDITOR

## Structural Modeling in the Mo–Bi–O System

Laura E. Depero and Luigi Sangaletti

*Dipartimento di Chimica e Fisica per i Materiali, Università di Brescia, Via Branze 38, 25123 Brescia, Italy*

Communicated by J. W. Richardson, August 15, 1995; accepted August 21, 1995

**A new approach is proposed for the structural study of inorganic compounds based on the search of the common features detectable in the cation sublattice distribution and applied to the Mo–Bi–O ternary system. In the diffraction patterns of these materials, as well as in many other ternary systems of bismuth oxide, a common feature is found in the presence of the strong reflection at about  $2\theta = 28^\circ$  ( $d = 3.2 \text{ \AA}$ ). Analogies and differences in the planes corresponding to this distance, which show a hexagonal net composed of Bi and Mo ions and, in some cases, structural vacancies, are discussed including also preliminary remarks on the possible effects of metal–metal interactions. The position of oxygen atoms with respect to the metal layers is also discussed in order to point out the structural features which allow the application of these materials as catalysts or gas sensors.** © 1995 Academic Press, Inc.

In order to understand the origin of the physical properties of complex oxide phases, it is basic to derive structural models revealing analogies and differences among these phases. Indeed, the comparison of the structural properties of complex oxides in terms of coordination polyhedra may be a difficult task due to the different coordination of metal cations with oxygen. Here a new approach is proposed for the structural study of inorganic compounds based on the search of the common features detectable in the cation sublattice distribution and applied to the Mo–Bi–O ternary system. This model also allows identification of planes in the structure parallel to the metal net, where oxygen ions can be easily available for catalysis and sensor applications. Indeed, bismuth molybdates are active and selective catalysts for the oxidation of propene (1), for the ammoxidation of propylene (2), and for CO oxidation (3). In this respect, the oxygen sublattice plays a major role, being the mechanism of catalysis related to the rapid diffusion of lattice oxygen atoms from the bulk to the catalyst surface. In addition, selectivity requires the catalyst structure to allow an easy removal and addition of oxygen (4). Bismuth molybdates have also been used as gas sensors. Indeed, the

oxygen vacancies are highly mobile at temperatures approaching  $400^\circ\text{C}$  and act as donors, thus having an immediate effect on the bulk conductivity (5).

The present approach has been recently applied to pure Bi–O phases to describe the  $\alpha$  to  $\beta$  and the  $\beta$  to  $\delta$  phase transitions as disorder–order transformations in the cation sublattice (6). The basic idea is that the high temperature phase can be derived by introducing a structural (static) disorder to the phase which is stable at the lowest temperature. Supporting this view there is the fact that, for example, in the cases of  $\text{Bi}_2\text{O}_3$  (7, 8),  $\text{ZrO}_2$  (9), and  $\text{WO}_3$  (10, 11) the high temperature phases can be stabilized by the presence of impurities.

The structures of three phases in the Bi–Mo–O system are known:  $\text{Bi}_2\text{Mo}_3\text{O}_{12}$ ,  $\text{Bi}_2\text{Mo}_2\text{O}_9$ , and  $\text{Bi}_2\text{MoO}_6$  (12). Although the  $\text{Bi}_2\text{O}_3$  phase diagram has been examined by a number of groups (13–17), most of the reported phases have unknown structures, since the metal stoichiometry appears sometime questionable (18). The diffraction patterns of  $\text{MoO}_3$ ,  $\text{Bi}_2\text{Mo}_3\text{O}_{12}$ ,  $\text{Bi}_2\text{Mo}_2\text{O}_9$ ,  $\text{Bi}_2\text{MoO}_6$ , and  $\alpha$ - and  $\beta$ - $\text{Bi}_2\text{O}_3$  have been simulated on the basis of the ICSD database (12) and reported in Fig. 1 (19). In all these patterns a common feature is given by the presence of the strongest reflection at about  $2\theta = 28^\circ$  ( $d = 3.2 \text{ \AA}$ ). The oxygen atoms contribute little to the structure factors and, for this reason, the detected analogy in the patterns of Fig. 1 can be attributed only to the similarities in the corresponding cation sublattices. Indeed, the strongest reflection, at about  $d = 3.2 \text{ \AA}$ , corresponds to the interplanar distance of a family of planes containing the cations. The projections of a single plane of the cation sublattices for  $\beta$ - $\text{Bi}_2\text{O}_3$  and the three Mo–Bi mixed oxide phases are shown in Fig. 2. In all these phases a hexagonal net can be identified. In the  $\text{Bi}_2\text{MoO}_6$  phase the distribution of the cation is the same as that in  $\beta$ - $\text{Bi}_2\text{O}_3$ , but, since two different cations are present in this ternary structure, their ordering changes the periodicity within the layer. The same hexagonal net is also present in the  $\text{Bi}_2\text{Mo}_2\text{O}_9$  and  $\text{Bi}_2\text{Mo}_3\text{O}_{12}$  structures, if structural vacancies are considered.

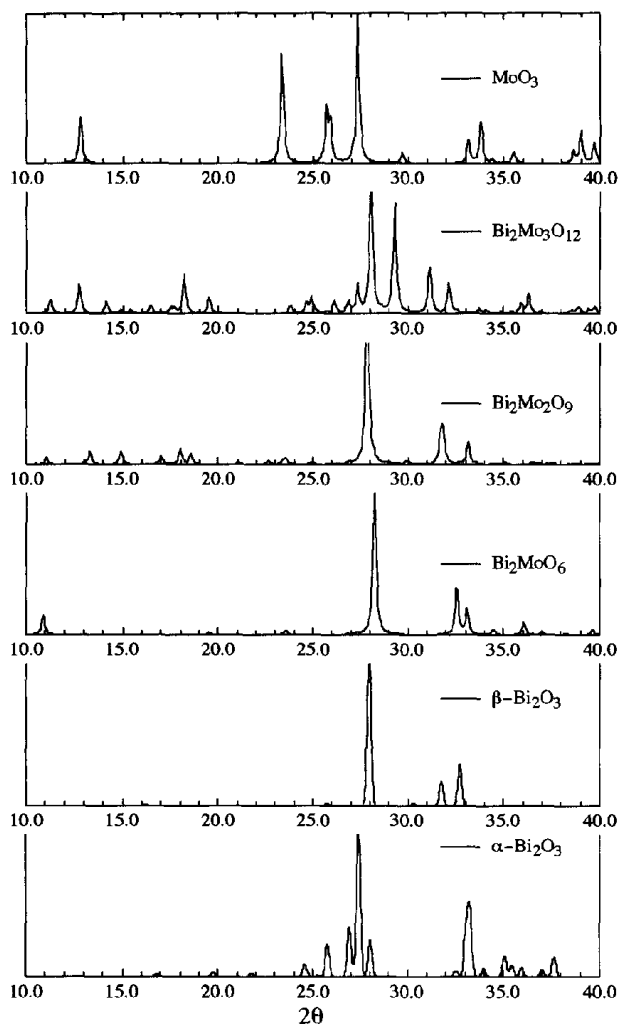


FIG. 1. Diffraction patterns of  $\text{MoO}_3$ ,  $\text{Bi}_2\text{Mo}_3\text{O}_{12}$ ,  $\text{Bi}_2\text{Mo}_2\text{O}_9$ ,  $\text{Bi}_2\text{MoO}_6$ ,  $\beta\text{-Bi}_2\text{O}_3$ , and  $\alpha\text{-Bi}_2\text{O}_3$ . In all these patterns a common feature is given by the presence of the strongest reflection at about  $2\theta = 28^\circ$  ( $d = 3.2 \text{ \AA}$ ).

In particular, one vacancy is present every 9 cation sites in the  $\text{Bi}_2\text{Mo}_2\text{O}_9$  cation layer, while in the  $\text{Bi}_2\text{Mo}_3\text{O}_{12}$  layer there are four structural vacancies every 24 cation sites.

The stoichiometry of all the mixed bismuth molybdenum oxides can be normalized to the formula  $\text{Bi}_x\text{Mo}_y\text{O}_{36}$ . In general, the charge balance relationship

$$3x + 6y = 2 \times 36 \quad [1]$$

must be satisfied. On the basis of this constraint, Table 1 has been derived, in which cation stoichiometry  $x$ ,  $y$  is related to the number  $n$  of structural vacancies according to the formula

$$n = 18 - (x + y). \quad [2]$$

It can be verified that  $n$ , as given in Table 1 for the observed structures, corresponds to the number of vacancies which can be found, by inspection, in the layers of Fig. 2. In the particular case of  $\text{Bi}_2\text{MoO}_6$ ,  $n = 0$  and, indeed, in this structure all cation sites are occupied in the layer (Fig. 2). The presence of vacancies in the other two reported structures can be rationalized with the hypothesis that for 18 cationic sites a maximum of 36 oxygen atoms can be inserted into the structure. In fact, when  $\text{Mo}^{6+}$  ions are substituted for  $\text{Bi}^{3+}$  ions in the cationic sites of  $\text{Bi}_2\text{MoO}_6$ , no more oxygen atoms can be inserted. As a consequence, in order to keep the charge balance, not all the cationic sites can be occupied.

In principle, as can be derived by inspection of Table 1, an infinite number of stoichiometric Bi:Mo ratios are

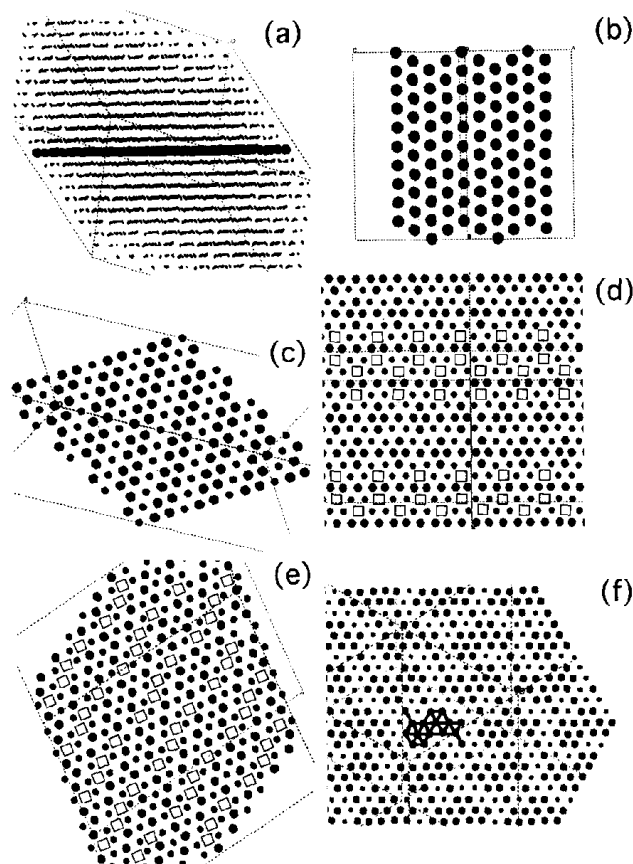


FIG. 2. (a) Lateral view of the  $22\bar{1}$  cation planes of  $\text{Bi}_2\text{Mo}_3\text{O}_{12}$  generating the strong reflection at  $d = 3.2 \text{ \AA}$  in the XRD spectrum. One single cation layer is also evidenced by a "ball" representation. This stacking of layers is representative of the cation layer stackings found in the other Mo-Bi-O phases which are similar to the present one and therefore are not reported. (b-f) Top view of the planes corresponding to the reflection at  $3.2 \text{ \AA}$  of  $\beta\text{-Bi}_2\text{O}_3$  -201- (b),  $\text{Bi}_2\text{MoO}_6$  -131- (c),  $\text{Bi}_2\text{Mo}_2\text{O}_9$  -023- (d),  $\text{Bi}_2\text{Mo}_3\text{O}_{12}$  -221- (e), and  $\text{Bi}_2\text{MoO}_6$ , high temperature phase -341- (f). The Bi atoms forming one cluster have been connected by straight lines. Where present, the vacancies have been evidenced by squares. Mo atoms are indicated by small balls, while Bi atoms are indicated by large balls.

**TABLE 1**  
**Relationship between the Cation Stoichiometry of  $\text{Bi}_x^{3+}\text{Mo}_y^{6+}\text{O}_{36}$  and the Number,  $n$ , of Structural Vacancies in the Cation Nets Shown in Fig. 2**

$x$	$y$	$x + y$	$n$	
0	12	12	6	$\text{MoO}_3$
1	11.5	12.5	5.5	
2	11	13	5	
3	10.5	13.5	4.5	
4	10	14	4	
5	9.5	14.5	3.5	
6	9	15	3	$\text{Bi}_2\text{Mo}_3\text{O}_{12}$
7	8.5	15.5	2.5	
8	8	16	2	$\text{Bi}_2\text{Mo}_2\text{O}_9$
9	7.5	16.5	1.5	
10	7	17	1	
11	6.5	17.5	0.5	
12	6	18	0	$\text{Bi}_2\text{MoO}_6$

possible. For  $y$  in the range 0 to 6, no vacancies are created when  $\text{Mo}^{6+}$  is substituted for  $\text{Bi}^{3+}$ , while, for  $y > 6$ , vacancies are necessarily present in order to keep the charge balance in the structure. As shown in Table 1, only the structures of the simplest stoichiometric ratios have been refined. This fact can be justified by the possible complexity of the structure required by the periodicity. Moreover, one can easily imagine a disordered situation in which the cation sites are statistically occupied by Mo and Bi, thus relieving the constraint imposed by the periodicity.

The same reasoning can be applied to the Bi–W–O system. With a very low content of  $\text{WO}_3$ , a  $\beta\text{-Bi}_2\text{O}_3$ -like solid solution was produced, while in  $\text{Bi}_{2-x}\text{W}_x\text{O}_{3+1.5x}$ , three ranges for solid solutions are reported, namely  $0.064 \leq x \leq 0.134$ ,  $0.134 < x < 0.186$ , and  $0.286 < x < 0.364$  (7).

In many inorganic compounds the metal atoms form clusters of different shapes and sizes; in particular, layers with a high concentration of metal atoms alternating with layers without metal atoms are known. As it was observed (20), metal–metal bonding may arise from a direct overlap of metal orbitals. Indirect interaction between metal atoms is also possible via a strongly polarizable medium consisting of either highly polarizable anions (insulators) or conduction electrons (metals). These interactions may lead to lattice distortions and clustering of metal atoms as well as to charge density waves.

The metal clustering in the present compounds may be related to some indirect metal–metal interactions. A close inspection of Fig. 3 shows a further common feature of the mixed Mo–Bi oxides in that Mo atoms always appear in pairs in the hexagonal cation net. Moreover, in the case of  $\text{Bi}_2\text{Mo}_3\text{O}_{12}$ , in addition to the Mo–Mo dimers, a peculiar “modulation” of the Mo distribution is present. The modulation can be identified by inspection of the planes corre-

sponding to the strong reflection at about  $2\theta = 29^\circ$ . In these planes, which contain all the cations of the lattice, the Mo atoms lay above and below the line identified by Bi atoms, with a modulation wavelength of about 37 Å (Fig. 3a). The modulation can be ascribed to the presence of Mo–O double bonds (Fig. 3b). Also the cation plane corresponding to this reflection (Fig. 3c) can be described by a hexagonal net similar to those shown in Fig. 2. Moreover, even in the recent structure refinement of the  $\text{Bi}_2\text{Mo}_3\text{O}_{12}$  high temperature form (18) the characteristic cation plane yielding the reflection at  $d = 3.2$  Å has a hexagonal net, but, when compared with the room temperature  $\text{Bi}_2\text{Mo}_3\text{O}_{12}$  phase, a clustering of Bi atoms is evident (Fig. 3f).

All these features indicate that metal–metal interactions in Mo–Bi–O compounds may play a relevant role in the determination of their physical properties and further investigations are needed to explore this subject. In general, it can be observed that a competition between a Bi–Mo substitutional disorder and cation clustering could be present in the metal sublattice. The regularity of cation distribution, which is found in the Bi–Mo hexagonal net of the compounds so far described, seems to indicate a prevalence of the clustering effect on disorder.

As for the oxygen content, which is important for the technological applications of Mo–Bi–O compounds, the possibility of substituting  $\text{Mo}^{6+}$  ions for  $\text{Bi}^{3+}$  ions in the  $\beta\text{-Bi}_2\text{O}_3$  layers means that in these layers a higher number of oxygen atoms can be inserted. Indeed, in  $\beta\text{-Bi}_2\text{O}_3$  there are 27 oxygen atoms for every 18 Bi atoms and therefore, in the structure, space is left for 9 more oxygen atoms. This observation can explain the fact that the ionic conductivity of the  $\delta\text{-Bi}_2\text{O}_3$  phase, recently described as derived by disordering the  $\beta\text{-Bi}_2\text{O}_3$  structure (6), is higher than that of  $\text{ZrO}_2$ . Indeed, even if the cation distribution in the two structures is the same, the smaller number of oxygen ions in  $\text{Bi}_2\text{O}_3$  may promote the ion diffusion.

The structural features of the oxygen sublattice are also important for the technological applications. It was shown that the ordering of the oxygen sublattice has a relevant role in the determination of the conduction properties of these materials (21–23). The properties of the oxygen sublattice must also be related to the previously discussed clustering and disorder of the hexagonal cation net. Substitutional disorder in the cation net may occur provided that the coordination constraints of Mo and Bi atoms with oxygen atoms are fulfilled. In this view, the difficulties encountered in determining by XRD the location of the oxygen atoms around metal sites in several Mo–Bi–O phases ( $\text{Bi}_6\text{Mo}_2\text{O}_{15}$  (24),  $13\text{Bi}_2\text{O}_3\text{--}10\text{MoO}_3$  (14), and  $\text{Bi}_{38}\text{Mo}_7\text{O}_{78}$  (25)) can be accounted for.

In conclusion, the present approach, which allows a systematic structural modelling of the Mo–Bi–O phases, can be extended to other mixed oxide families. This is the case of  $\text{BiNbO}_4$ ,  $\text{BiVO}_4$ ,  $\text{Bi}_2\text{PtO}_7$ ,  $\text{Bi}_8\text{La}_{10}\text{O}_{27}$ ,  $\text{Bi}_7\text{La}_3\text{O}_{15}$ , and

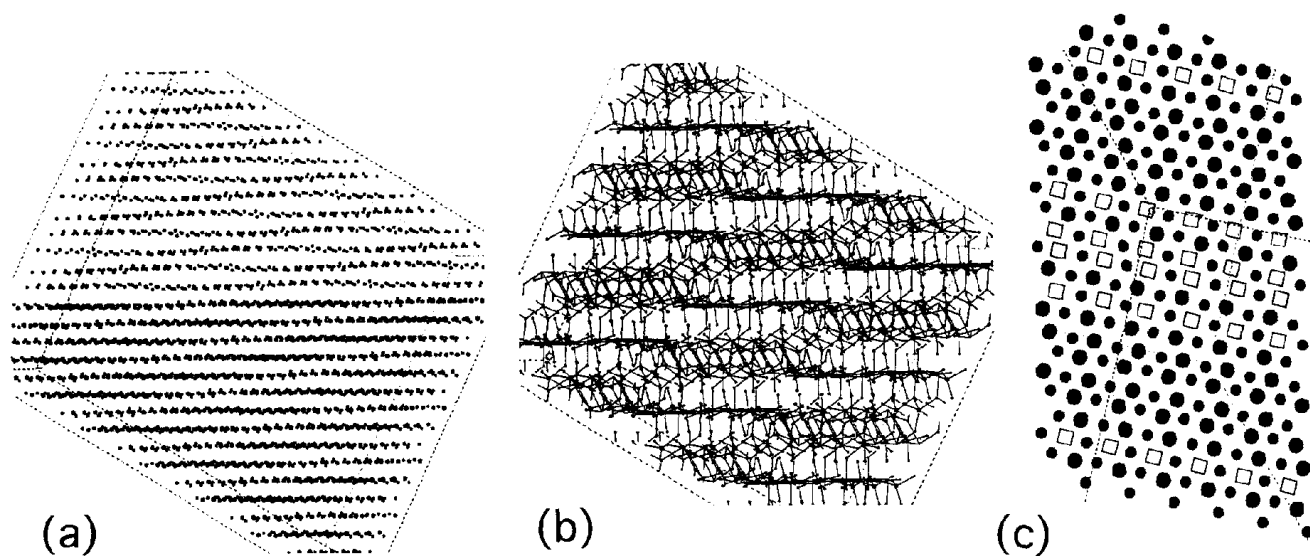


FIG. 3. (a) Lateral view of the 023 cation planes of  $\text{Bi}_2\text{Mo}_3\text{O}_{12}$ . In order to point out the Mo atoms modulation, in the upper half of the figure only the Mo atoms are shown. (b) Enlargement of the lateral view of the 023 planes with oxygen atoms included. The oxygen double bonding with Mo contributes the cation layer separation, while the cation layers are closer to each other when connected by bridging oxygen atoms. (c) Top view of the 023 planes. Also in this case, the hexagonal net of cations can be observed. Structural vacancies are indicated by squares. Mo atoms are indicated by small balls, while Bi atoms are indicated by large balls.

$\text{Bi}_4\text{V}_2\text{O}_{11}$  (12), where the characteristic strongest peak at  $d = 3.2 \text{ \AA}$  in the diffraction pattern is observed. Correspondingly, a similar stacking of cationic "hexagonal" nets can be identified. In these cases all the cation sites are occupied, since for 18 cations less than 36 oxygen atoms are always required.

The present approach may also be helpful in the interpretation of the diffraction patterns of thin film samples with substitutional elements in the cation sites (26). In this frame, these films could be properly described as compounds with local dishomogeneities in the stoichiometric ratio instead of materials with several phases separated by grain boundaries.

#### ACKNOWLEDGMENTS

We thank M. Zocchi and E. Tondello for useful discussions.

#### REFERENCES

1. T. Tsunoda, T. Hayakawa, T. Kameyama, and K. Takehira, *J. Chem. Soc. Faraday Trans.* **91**, 1117 (1995).
2. R. K. Grasselli and J. D. Burrington, *Adv. Catal.* **30**, 133 (1981).
3. D. H. Galvan, S. Fuentes, M. Avalosborja, L. Cotaariza, E. A. Early, M. B. Maple, and J. Cruzreyes, *J. Phys. Condens. Matter* **5**, A217 (1993).
4. C. N. R. Rao and J. Gopalakrishnan, "New Directions in Solid State Chemistry," p. 469. Cambridge Univ. Press, Cambridge, UK, 1986.
5. N. Hykaway, W. M. Sears, R. F. Frindt, and S. R. Morrison, *Sens. Actuators* **15**, 105 (1988).
6. L. E. Depero and L. Sangaletti, in preparation.
7. W. Zhou, *J. Solid State Chem.* **108**, 381 (1994).
8. D. Conflant, C. Follethouttemane, and M. Drache, *J. Mater. Chem.* **1**, 649 (1991).
9. L. E. Depero and P. Levrangi, *J. Solid State Chem.* **110**, 190 (1994).
10. L. E. Depero, S. Groppelli, I. Natali-Sora, L. Sangaletti, G. Sberveglieri, and E. Tondello, submitted for publication.
11. K. H. Cheng and M. S. Whittingham, *Solid State Ionics* **1**, 151 (1980).
12. ICSD Inorganic Crystal Structure Database, Release 95/1 FIZ-Fachinformationszentrum Karlsruhe and GMELIN Institut.
13. R. Kohlmuller and J. P. Badaud, *Bull. Soc. Chim. Fr.* **10**, 3434 (1969).
14. T. Chen and S. Smith, *J. Solid State Chem.* **13**, 288 (1975).
15. M. Egashira, K. Matsuo, S. Kagawa, and T. Seiyama, *J. Catal.* **58**, 409 (1979).
16. D. J. Buttrey, D. A. Jefferson, and J. M. Thomas, *Philos. Mag. A* **53**, 897 (1986).
17. F. D. Hardcastle and I. E. Wachs, *J. Phys. Chem.* **95**, 10763 (1991).
18. D. J. Buttrey, T. Vogt, U. Wildgruber, and W. R. Robinson, *J. Solid State Chem.* **111**, 118 (1994).
19. The results published were generated using the program CERIUSt. This program was developed by Molecular Simulations Incorporated.
20. C. Haas, *J. Solid State Chem.* **57**, 82 (1985).
21. J. Berezovsky, H. K. Liu, and S. X. Dou, *Solid State Ionics* **66**, 201 (1993).
22. K. Z. Fung, J. Chen, and A. V. Virkar, *J. Am. Ceram. Soc.* **76**, 2403 (1993).
23. G. Chiodelli, A. Magistris, G. Spinolo, C. Tomasi, V. Antonucci, and N. Giordano, *Solid State Ionics* **74**, 37 (1994).
24. S. Miyazawa, A. Kawana, and H. Koizumi, *Mater. Res. Bull.* **9**, 41 (1974).
25. D. J. Buttrey, D. A. Jefferson, and J. M. Thomas, *Mater. Res. Bull.* **21**, 739 (1985).
26. L. E. Depero, L. Sangaletti, M. Zocchi, and G. A. Rizzi, "Proceedings of the Congress on Perspectives in Inorganic Chemistry, Bressanone, Italy, October 2-7, 1994," in press.